Quantitative Assessment of Neurons and Neuroglia with Computer Morphometry

R. M. Khudoerkov and D. N. Voronkov

Translated from *Byulleten' Eksperimental'noi Biologii i Meditsiny*, Vol. 149, No. 1, pp. 109-112, January, 2010
Original article submitted July 1, 2009

The morphology of neural and glial cells in different cerebral areas and in various experimental models was quantitatively studied by methods of computer morphometry combined with video image analysis systems. The following parameters were obtained: density of neurons and glial cells per 1 mm^2, number of satellite perineuronal glial cells, aspect ratio for neural and glial cells, the area occupied by neuroglial projections, *etc*. The tested computer morphometry methods can be efficient in quantitative assessment of pathological and regenerative processes in the nervous tissue.

Key Words: *morphometry; image analysis; brain; neuron; neuroglia*

Apart for maintenance of normal function of neurons, neuroglia interacts with them as equal members at the neurotransmitter and metabolic levels [9,13]. Therefore, the search for novel methodical approaches to the study of structural and functional peculiarities of neurons and glial cells with the help of computer morphology not only widens our views on the fundamental principles of brain functioning, but also contributes to the knowledge of compensatory and reparative reactions during the development of pathological processes.

Our aim was to adapt the methods of computer-aided image analysis in order to quantify the distribution of neurons and glial cells in histological sections and assess their role in the diagnosis of pathological and compensatory-reparative alterations in brain structures.

MATERIALS AND METHODS

The experiments were carried out on paraffin sections (7 μ) of rat and guinea pig brain fixed in Carnoy fluid and stained by the Nissl method. Glial fibrillary acidic protein (GFAP) was detected in astrocytes by enzyme immunoassay [12] with rabbit monoclonal antibodies (Sigma) according to manufacturer's protocol. Secondary biotinylated goat antibodies and avidin-peroxidase detection with 3,3-diaminobenzidine (Sigma) were used for visualization.

For morphometry, the cerebral sections were photographed using a Leica DMLB microscope (×40) and a Leica DC-300 digital camera (3.2 Mpix). The digital images were stored in TIFF format with maximum resolving power and shown on a display for processing and analysis. The automated image analysis was performed with a Leica QWin [11] and ImageJ [8] software. Manual selection of the objects was carried out with a Wacom graphic tablet.

The function realized in the software analyzing the histological images are based on mathematical morphology methods [2,3]. Analysis of video images can be subdivided into several basic steps: *a*) primary processing with tracing of the examined regions, zooming of this region, color correction, video noise suppression, *etc*.; *b*) segmentation, *i.e.* isolation of the examined objects in the image using manual or automated procedure; statistical processing and analysis of the data obtained.

The functions of video analyzing software assess the quantitative parameters of the cellular elements in

Laboratory of Functional Morphochemistry, Neurology Research Center, Russian Academy of Medical Sciences, Moscow, Russia. ***Address for correspondence:*** rolfbrain@yandex.ru. R. M. Khudoerkov

the brain: the number of neural and glial cells in the microscope visual field and their relative content, the number of perineural glial cells, and the area of the profile field of the soma, cytoplasm, and nucleus of the cell elements. In addition, it can assess the shape of the soma and nucleus in neural and glial cells, measure the length of projections, calculate the area occupied by neuroglial projections, and measure the distance of neuroglia from the neurons and vessels.

RESULTS

Perineural glial elements were counted using Expansion Function. In the graphic tablet, a mask was manually applied to a neuron, which traced a closed contour along the somatic perimeter. The neuroglia nuclei visible in microscope vision field were covered with the masks using ellipse-approximating functions (Fig. 1, *a*). Then, the neuron mask was automatically widened with the Expansion Function by two average diameter of glial cell nucleus. The number of neuroglial cells was determined within this expanded mask. The above method of perineural glia count combined with measurement of the area of the profile field of neuron soma was tested in the experiment on sensorimotor cortex of guinea pigs. It could assess the peculiarities of distribution of various type neurons in the cortical layer V by the number of satellite gliocytes and made it possible to reveal morphological correlates of neurons with their functional heterogeneity revealed by electrophysiological measurements [5].

The image analysis programs greatly facilitates counting of the total number of neural and glial cells in the microscope visual field, assessment of the number of cells per 1 mm^2, and calculation of the neuroglial index, *i.e.* glial cells/neurons ratio per unit area. The number of neural and glial cells in the visual microscopic field (*i.e.*, in the isolated region of interest) can be determined automatically usig Segmentation Function by the level of brightness or by manual isolation of the objects. In the study of protective effects of preconditioning against acute ischemic lesions to the brain carried out on the model of local cerebral infarction in rats we showed that this preconditioning decreased the neuroglial index in the perifocal infarction area by 25%. This attests to moderation of the inflammatory processes in the damaged area and activation of compensatory and reparative processes [1]. In experiments with excessive loading the rats with L-DOPA, the neuroglial index made it possible to assess the degree of involvement of various type neurons in the sensorimotor cortex and striatum into dysfunction of the dopaminergic system [7].

The shape of the objects such as cell soma or nucleus can be characterized by a function describing the shape factors. This function can calculate: *a*) roundness, a parameter assuming minimum value of 1 for a circle; *b*) shape index that shows the convexity or concavity of the cell body; *c*) aspect ratio equal to the ratio of long to short axes of the cell body characterizing its elongation. During analysis of neuron shape in rat striatum, the aspect ratio parameter quantitatively evaluated the elongation of the neuron bodies caused by injection of 3-nitropropionic acid (mitochondrial toxin). Moreover, this parameter reflected normalization of neuron roundness accompanied by other compensatory and reparative manifestations induced by intraventricular injection of the stromal cell suspension from the adipose tissue to rats [4]. Aspect ratio was further employed to analyze the effect of overloading the dopaminergic system in rat brain with L-DOPA on the shape of neuroglial nuclei in the nigrostriatal structures such as substance nigra and striatum. Glial cell nuclei were more deformed by L-DOPA in the substantia nigra than in the striatum [6].

The spreading area of neuroglial projection was assessed in the astrocytic preparations with GFAP visualized by immune essay. To this end, a closed contour was manually drawn around the astrocyte arborization, which passed over the terminal branches of the projections and formed a convex polygon (Fig. 1, *b*). This polygon could be also obtained in the automated mode by combined application of Segmentation and Convex Hull Functions according to brightness of the object. In this polygon, the area and aspect ratio were determined. The first parameter assessed the area occupied by neuroglial projections, while the second one described elongation of the cell soma.

TABLE 1. Area Occupied by Neuroglial Projections and Aspect Ratio of GFAP-Positive Glial Cells in *Fascia Dentata* of Rat Hippocampus

Hippocampal fascia dentata	Area of astrocytic projections μ^2	Aspect ratio
Polymorphic layer	351±10.1	1.52±0.02
Molecular layer	865±35.1*	2.33±0.06*

Note. *$p<0.05$ compared to polymorphic layer (Mann–Whitney test).

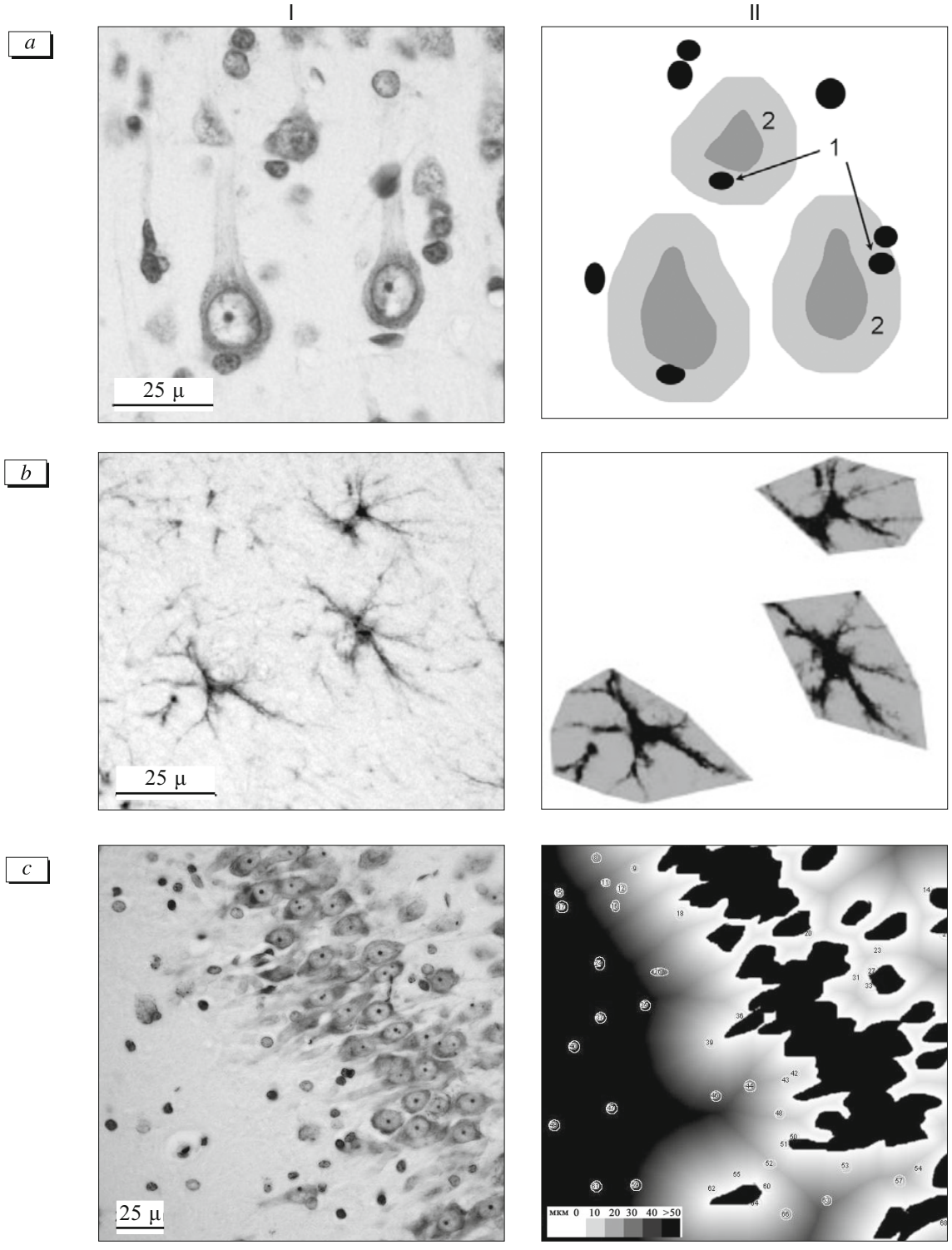

Fig. 1. Application of morphometry methods to yield the quantitative parameters of the cellular elements in the brain. *I*) Nervous tissue of rat brain obtained with a Leica DMLB light microscope and a Leica DC-3000 digital camera with an ×40 objective. *II*) image analysis procedures during morphometry of cerebral structures; a) frontoparietal cortex of rat brain, layer V; Nissl staining; the neuron bodies were covered with corresponding masks under Expansion Function, thereafter the perineural glial cells (*1*) were counted within the limits of expanded neuron mask (*2*); *b*) frontoparietal cortex of rat brain, layer V; immunohistochemical method to detect GFAP in astrocytes; measurement of astrocytic projections area under the combined use of Segmentation and Convex Hull Functions according to brightness of the objects; *c*) field CA_3 of rat brain hippocampus, Nissl staining; Distance Map Function was used to measure the distance from neuroglia to the neurons. The darker the gray scale brightness of a region, the larger the distance between the neuroglial and neuron masks.

As an example, we present morphometry data of GFAP-positive glial cells in polymorphic and molecular layers of hippocampal fascia dentata in intact Wistar rats. In three rats, 100 glial cells were examined in each layer. In the molecular layer, the area and aspect ratio (characterizing elongation of the shape) were higher by 2.5 and 1.5 times, respectively, compared to the corresponding parameters in the polymorphic layer (Table 1). The morphometry data clearly revealed quantitative differences in the structural organization of neuroglia in the polymorphic and molecular layers of hippocampal *fascia dentata*.

The methods of video analysis enables not only measuring of the spreading area of astrocytic projections, but also assessing the intensity of the immune reaction to GFAP using Total Brightness Function (the sum of brightness of all pixels in the image) thereby evaluating the degree of GFAP expansion in the cell [10].

The distance from glial cells to neurons was measured using Distance Map Function on sections stained by the method of Nissl. To this end, the bodies of neurons and glial cells were covered by the corresponding masks, while the brightness of gray scale between the neuron masks was set proportional to the distance between neuroglial and neuronal masks (Fig. 1, *c*). This approach transformed brightness into distance with Measure Gray Mean Function. In addition to characterization of remoteness of the glial cells from neurons, the determined distance made it possible to subdivide glia into free and perineural fractions and to analyze spatial glial redistribution. The Distance Map Function can be employed for calculation of the distance between glial cells and other cerebral structures.

Thus, the methods of digital image analysis of neurohistological structures not only quicken and facilitate determination of a number of quantitative parameters of neurons and glial cells, but they also open new vista in morphological characterization of examined objects. Overall, these methods widen the possibilities to assess quantitatively the morphological parameters of the pathological processes and compensatory-reparative alterations in the brain.

REFERENCES

1. S. A. Gavrilova, N. S. Samoilenkova, Yu. A. Pirogov, *et al., Patogenez*, **6**, No. 3, 13-17 (2008).
2. R. Gonzales, R. Woods and S. Eddins, *Digital Image Processing with Matlab* [in Russian], Moscow (2006).
3. A. R. Clarke and C. N. Eberhard, Microscopy Techniques for Materials Science [in Russian] Moscow (2007).
4. A. V. Kulikov, M. S. Stepanova, S. L. Stvolinskii, *et al., Klet. Tekhnol. Biol. Med.,* No. 2, 83-89 (2008).
5. Yu. S. Mednikova, N. V. Pasikova, A. V. Rogal', *et al.,* Actual Problems of Functional and Interhemispheric Asymmetry and Neuroplasticity, Moscow (2008), pp. 465-469.
6. R. M. Khudoerkov and D. N. Voronkov, *Structural and Functional Neurochemical and Immunochemical Regularities in Brain Asymmetry and Plasticity*, Moscow (2007), pp. 665-670.
7. R. M. Khudoerkov, E. L. Dovedova, and D. N. Voronkov, *Byull. Eksp. Biol. Med.,* **144**, No. 7, 39-41 (2007).
8. M. D. Abramoff, P. J. Magellhaes, and S. J. Ram, *Biophot. Int*., **11**, No. 7, 36-42 (2004).
9. E. E. Benarroch, *Mayo Clin. Proc*., **80**, No. 10, 1326-1338 (2005).
10. E. M. Brey, Z. Lalani, C. Johnston, *et al., J. Histochem. Cytochem*., **51**, No. 5, 575-584 (2003).
11. *Leica Qwin Reference Guide*, Cambridge (1996).
12. J. P. O'Callaghan and K. Sriram, *Expert Opin. Drug Saf*., **4**, No. 3, 433-442 (2005).
13. A. Verkhratsky and A. Butt, *Glial Neurobiology: A Textbook*, West Sussex (2007).